A Unified Theory of Ionosphere-Plasmasphere Transport of Suprathermal Electrons

George V. Khazanov, Torsten Neubert, and Grigorii D. Gefan

Abstract— **We present a model of suprathermal electrons in the ionosphere and plasmasphere based on a solution to the kinetic equation along the entire length of a closed magnetic field line, that is, simultaneously for the two conjugate ionospheres and the plasmasphere. We call this the unified approach. It allows the determination of the distribution in energy and pitch-angle of photoelectrons along the complete length of the field line thereby avoiding the introduction of artificial boundaries between the ionosphere and magnetosphere and, consequently, avoids problems introduced by the uncertainty of these boundary conditions. In addition, it automatically accounts for back-scattered electrons in the atmosphere and plasmasphere, and avoids splitting photoelectrons into a loss-cone and a trapped population. The method is not limited to specific situations such as conjugated sunrise or symmetrical illumination of hemispheres, but is equally applicable to arbitrary illumination conditions.**

I. Introduction

SUPRATHERMAL electrons (1 eV–500 eV) are formed predominantly by two processes: photoionization of the Earth's atmosphere by solar radiation, and impact ionization of the neutral atmospheric constituents by high energy (1–10 keV) electrons of magnetospheric origin. In order to study such phenomena as the heating of the thermal ionospheric and plasmaspheric plasma, optical emissions in the upper atmosphere, and the stability of the ionospheric plasma, the distribution function of suprathermal electrons must be known.

The maximum production rate is approximately at 150 km altitude for photoelectrons, while the altitude of secondary electron production from impact ionization depends on the energy spectrum of the precipitating energetic electrons. The altitude of maximum ionization is shifted deeper into the atmosphere when the energy of the precipitating electrons increases. The latter process prevails at high latitudes and stimulates polar lights (aurora).

Suprathermal electrons created in the ionosphere below about 250 km lose their energy locally due to the high density of neutral particles (short mean free path). As a result, the distribution function is close to isotropic. The main challenge is the calculation of all the inelastic processes that, together with the source spectrum, determine the fine structure of the electron energy spectrum. In particular, there are sharp photoionization peaks in the photoelectron spectrum in the interval 25–30 eV and a characteristic trough at energies less than 4 eV, which is associated with a large cross-section of the vibrational excitation of molecular nitrogen.

In the upper ionosphere, above 250 km, transport processes begin to play a substantial role. A fraction of suprathermal electrons generated at these altitudes will have sufficient energy to escape the atmosphere along the magnetic field and stream into the magnetosphere. A self-consistent model for the transport of suprathermal electrons on closed magnetic field lines must consider particle exchange between magnetic conjugate regions. However, most theories developed in the past, simplified the nature of this exchange. One assumption often used in photoelectron production models was to neglect contributions from incoming electrons at high altitudes. This scenario assumes not only the absence of ionization in the conjugate hemisphere, but also an unrealistic small role of the back-scattering of particles. Alternative methods defined an upper boundary condition using sounding rocket or satellite observations of electron energy spectra at high altitudes. With relatively little interest in the problem of interactions between conjugate regions, the main attention was focused on three aspects: (1) the source (photo- and secondary ionization), (2) collisional relaxation of precipitating electrons, and (3) transport of suprathermal electrons from the source region. In the following we review the most common approaches used to address these problems.

The simplest of the discrete energy-loss approaches is the local equilibrium approximation (e.g., [1]–[3]) in which the photoelectron flux is determined solely from local production and loss mechanisms. The calculation assumes altitudes sufficiently deep in the atmosphere so that transport effects are negligible. However, for altitudes above 250 km, a versatile approach to the transport problem is given by linear transport theory, in which the essential physics of electron-atmosphere interactions can be accommodated. Linear transport theory provides a unified description in both the local equilibrium and transport dominated regimes. Many models have been developed to describe the transport and energy degradation process of photoelectrons [4]–[10] as well as the transport theory for the auroral electron problem [11]–[24]. Monte-Carlo methods were also used to describe the interaction of precipitating electrons with the atmosphere [25]–[27], and photoelectron fluxes [28].

Efforts to extend models to include effects of photoelectron fluxes arriving from the conjugate hemisphere caused the appearance of papers studying the transport of photoelectrons in the plasmasphere. Since Coulomb collisions of suprathermal electrons with thermal electrons and ions are rare in this region, it was thought at first that photoelectrons pass through the plas-

Manuscript received March 22, 1993; revised January 12, 1994. This work was supported by NASA grants NAGW-1619, NAG5-1500 and contract NAS8-35350, and NSF grant ATM-9114409.

G. V. Khazanov and T. Neubert are with the Space Physics Research Laboratory, Department of Oceanic, Atmospheric and Space Science, University of Michigan, Ann Arbor, MI 48109-2143.

G. D. Gefan is with the Irkutsk Polytechnical Institute, Irkutsk, Russia.

IEEE Log Number 9216614.

masphere almost freely. In that case, diffusion in energy and pitch-angle could be ignored [29]. However, the discrepancy between observed distributions and those calculated under these assumptions made [30] consider particle trapping effects induced by the magnetic mirror force of the Earth's dipole magnetic field. Later, [31] and [32] gave some qualitative discussion of electron trapping and the resulting increase in plasmaspheric heating.

That marked the beginning of the second stage of research, when it was attempted to perform a quantitative analysis of suprathermal electrons in the plasmasphere. Calculations were made of the transparency of the plasmasphere relative to particle and energy flux, as well as heating rates of thermal electrons by photoelectrons, using Monte-Carlo methods [33], by solving the kinetic equation numerically [34], and through analytical methods [35]–[37].

Parallel to these studies were efforts attempting to describe the dynamics of suprathermal electrons with the participation of both hemispheres [38]. However, at that time techniques were not yet developed to accurately take into account the effect of the plasmaspheric transport of suprathermal electrons. When these were developed as described above, it became possible to create combined methods, which accounted for photoelectron fluxes coming from magneto-conjugate regions. That became the subject of the third stage of investigations, when the models by [39]–[41] were developed. However, certain limitations remained, which did not allow the examination of other effects caused by suprathermal electrons:

1) The foundations of the combined methods mentioned above is to determine the flux in the ionosphere using coefficients of the plasmaspheric transparency which are calculated independently. With such an approach one introduces artificial boundaries between the ionosphere and plasmasphere, and between the population of loss-cone electrons and trapped electrons. Consequently, the calculation of the electron distribution function near these artificial boundaries rests on *a priori* assumptions and is sensitive to the imposed boundary conditions.
2) All studies referenced above determined time-stationary solutions. This approximation is a serious constraint and does not allow the study of the response of the complete system to sunrise and sunset conditions, as well as to natural and artificial injection of energetic electrons.
3) The study of the processes associated with the excitation of plasma oscillations and their interaction with suprathermal electrons remained unfinished.

In this paper, we present a new model which includes item 1, while effects of non-stationary solutions and plasma instabilities will be considered in separate papers. In Section 2, the kinetic equation is derived with expressions for the collisional terms given in the appendix. In Section 3 we study ionospheric-plasmaspheric transport of photoelectrons. To illustrate the problems associated with a separate treatment of the ionosphere and the magnetosphere, as frequently done, the model is first applied to these regions separately, then to the complete system. Finally, Section 4 contains a discussion and a summary.

II. The Kinetic Equation for Suprathermal Electrons

Non-Maxwellian electrons in the Earth's ionosphere and plasmasphere can be described by the Boltzmann kinetic equation

$$\frac{\partial f}{\partial t} + \vec{v}\vec{\nabla} f - \frac{e}{m}\left(\vec{E} + \frac{\vec{v}\times\vec{B}}{c}\right)\vec{\nabla}_{\vec{v}} f = S_{ee} + \sum_i \left(S_{ei} + S^*_{ei} + S^-_{ei}\right) + \sum_\alpha \left(S_{e\alpha} + S^*_{e\alpha} + S^+_{e\alpha}\right) + q \quad (1)$$

where $f = f(t, \vec{r}, \vec{v})$ is the electron velocity distribution function, $\vec{B}, \vec{E}$ magnetic and electric fields, S_{ee} describes collisions with Maxwellian electrons, S_{ei} and $S_{e\alpha}$ elastic collisions with ion and neutral species i, α, S^*_{ei} and $S^*_{e\alpha}$ excitation of ion and neutral species, $S^+_{e\alpha}$ and S^-_{ei} ionization and recombination, and q the source of photoelectrons.

Let us introduce a coordinate system $[t, E, s, \theta, \phi]$, where E is the electron energy, s is the coordinate along the geomagnetic field line, θ the electron pitch-angle and ϕ the azimuth angle. The differential flux $\psi = 2Ef/m^2$, is defined in such a way that $\psi(t, E, s, \theta, \phi)dEd\Omega$ is the flux of electrons with energy from E to $E + dE$ inside a solid angle $d\Omega = \sin\theta d\theta d\phi$ around (θ, ϕ) at a point s along the field.

In the domain considered here, the electron cyclotron period is small compared to other characteristic time scales, and the electron Larmor radius is small compared to the gradients of the geomagnetic field. This allows the use of the guiding center approximation in which case (neglecting the drift across the geomagnetic field), (1) can be expressed as [59]

$$\frac{\beta}{\sqrt{E}}\frac{\partial\psi}{\partial t} + \mu\frac{\partial\psi}{\partial s} - \frac{1-\mu^2}{2}\left(-\frac{F}{E} + \frac{1}{B}\frac{\partial B}{\partial s}\right)\frac{\partial\psi}{\partial\mu} + EF\mu\frac{\partial}{\partial E}\left(\frac{\phi}{E}\right) = \langle S\rangle \quad (2)$$

Here, the energy E is measured in eV, the constant $\beta = 1.7 \times 10^{-8}\mathrm{eV}^{1/2}$ cm^{-1}s, and $\mu = \cos\theta$. The force due to the longitudinal electric field is $F = -eE_\parallel$ and is expressed in units of eVcm^{-1}. The right hand side of (1), averaged over azimuth angle, is expressed on symbolic form by $\langle S\rangle$. The collision terms are described in some detail in the appendix. With (3a), (5a), (8a), (9a) the kinetic equation (1) can now be expressed as

$$\begin{aligned}\frac{\beta}{\sqrt{E}}\frac{\partial\psi}{\partial t} + \mu\frac{\partial\psi}{\partial s} = {} & \frac{1-\mu^2}{2}\left(-\frac{F}{E} + \frac{1}{B}\frac{\partial B}{\partial s}\right)\frac{\partial\psi}{\partial\mu} \\ & + (An_e - EF\mu)\frac{\partial}{\partial E}\left(\frac{\psi}{E}\right) \\ & + \frac{1}{2}\left(\frac{An_e}{E^2} + \sum_\alpha n_\alpha\sigma^{(1)}_\alpha\right)\frac{\partial}{\partial\mu}\left[(1-\mu^2)\frac{\partial\psi}{\partial\mu}\right] \\ & + \sum_\alpha n_\alpha \sum_j E^*_{\alpha j}\frac{\partial}{\partial E}(\sigma^*_{\alpha j}\psi) \\ & + \sum_\alpha n_\alpha\left\{\frac{\partial}{\partial E}\left[\sigma^+_\alpha\psi(E^+_\alpha + \langle E\rangle_\alpha)\right]\right. \\ & \left. + \int_{2E+E^+_\alpha}^{\infty} I^+_\alpha(E', E)\psi_0 dE'\right\} + Q(E, \mu, s)\end{aligned} \quad (3)$$

where Q is the electron production rate due to processes other than electron impact ionization in units of cm^{-3} eV^{-1} $ster^{-1}$ s^{-1}.

III. Ionosphere-Plasmasphere Transport of Photoelectrons

The method described below is based on a solution to the kinetic equation along the entire length of a closed magnetic field line, that is, simultaneously for the two conjugate ionospheres and the plasmasphere. We call this the unified approach. It allows the determination of the distribution in energy and pitch-angle of photoelectrons along the complete length of the field line thereby avoiding the introduction of artificial boundaries between the ionosphere and magnetosphere and, consequently, avoids problems introduced by the uncertainty of these boundary conditions. In addition, it automatically accounts for back-scattered electrons in the atmosphere and plasmasphere, and avoids splitting photoelectrons into a loss-cone and a trapped population. The method is not limited to specific situations such as conjugated sunrise or symmetrical illumination of hemispheres, but is equally applicable to arbitrary illumination conditions.

Along a closed magnetic field line in the plasmasphere, the magnetic field is strongly inhomogeneous, while collisional diffusion terms are small due to the long mean free path. In order to decrease undesirable computational effects associated with approximation errors of the derivatives $\partial/\partial s$ and $\partial/\partial\mu$, it is convenient to change variables from (μ, s) to (μ_o, s), where

$$\mu_o = \frac{\mu}{|\mu|}\sqrt{1 - \frac{B_o}{B}(1-\mu^2)} \tag{4}$$

with B_o and μ_o denoting the magnetic field and the cosine of the pitch-angle at the magnetic equator of the flux-tube. This change of variables is desirable because $\psi(\mu_o, s)$ now is a slowly varying function with s (μ_o is the adiabatic invariant). For the stationary case with no electric fields, (3) becomes

$$\begin{aligned}\mu\frac{\partial\psi}{\partial s} = {} & \frac{1}{2}\left(\sum_\alpha n_\epsilon \sigma_\alpha^{(1)} + \frac{An_\epsilon}{E^2}\right) \\ & \times\left[\frac{(1-\mu_o^2)(B_o/B - 1 + \mu_o^2)}{\mu_o^2}\frac{\partial^2\psi}{\partial\mu_o^2}\right. \\ & \left.+\frac{\mu_o^2 - 2\mu_o^4 + 1 - (\mu_o^2+1)B_o/B}{\mu_o}\frac{\partial\psi}{\partial\mu_o}\right] \\ & + An_\epsilon\frac{\partial}{\partial E}\left(\frac{\psi}{E}\right) + \sum_\alpha n_\alpha \sum_j E_{\alpha j}^*\frac{\partial}{\partial E}(\sigma_{\alpha j}^*\psi) \\ & + \sum_\alpha n_\alpha\left\{\frac{\partial}{\partial E}[\sigma_\alpha^+\psi(E_\alpha^+ + \langle E\rangle_\alpha)]\right. \\ & \left.+\int_{2E+E_\alpha^+}^{\infty} I_\alpha^+(E', E)\psi_0 dE'\right\} + Q \end{aligned} \tag{5}$$

The new variable μ_o takes on values in the range $|\mu_{oB}| < |\mu_o| < 1$, where the lower boundary $\mu_{oB} = \sqrt{1 - B_o/B(s)}$ is a function of s. A specific feature of the algorithm used to solve (5) is that the number of grid points in μ_o varies with s because the definition interval varies with s. In the magnetosphere, where the inhomogeneity of the magnetic field causes μ_{oB} to vary significantly, the number of steps in μ_o is increased by 2 for each step in s towards the magnetic equator. This scheme is illustrated in Fig. 1, which shows the adopted grid as function of s and $\theta_o = \cos^{-1}\mu_o$. Since the magnetic field changes little in the ionosphere, while at the same time the step size in s is smaller in this region, the values of μ_{oB} at adjacent altitude grid points would be undesirably close if this scheme was extended all the way to the base of the ionosphere. Instead, we assume that the magnetic field is homogeneous below some altitude s_1 (typically 1000 km) so that μ_{oB} is constant in the ionosphere.

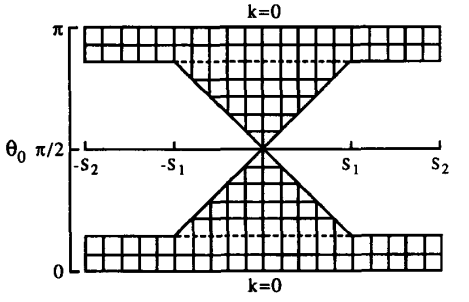

Fig. 1. The region in (θ_o, s) where ψ is defined. The dashed lines indicate the loss-cone boundary, $\pm s_1$ define the boundaries between the two conjugate ionospheres and the magnetosphere and $\pm s_2$ define the lower boundary in the ionosphere.

In Fig. 1, dashed lines indicate the loss cone boundary $\mu_o = \pm\sqrt{1 - B_o/B(s_1)}$. The number of grid points in the loss cone is constant for the complete field line. The trapping region is defined by $\sqrt{1 - B_o/B(s)} < |\mu_o| < \sqrt{1 - B_o/B(s_1)}$ and the loss-cone region by $\sqrt{1 - B_o/B(s_1)} < |\mu_o| < 1$. The boundary conditions in s are imposed at conjugate points of the ionosphere, $-s_2$ and $+s_2$ at 90 km altitude using the local approximation ($\partial/\partial s = 0$). The boundary conditions in θ_o are [43]

$$\begin{aligned}\frac{\partial\psi(\theta_o = 0, \pi)}{\partial\theta_o} &= 0; \quad \theta_o = \cos^{-1}\mu_o \\ \psi^+(t, s, \mu_o = \mu_{ob}, E) &= \psi^-(t, s, \mu_o = -\mu_{ob}, E) \\ \frac{\partial\psi^+(t, s, \mu_o = \mu_{ob}, E)}{\partial\theta_o} &= -\frac{\partial\psi^-(t, s, \mu_o = -\mu_{ob}, E)}{\partial\theta_o}\end{aligned} \tag{6}$$

With a finite-difference approximation of the derivatives

$$\frac{\partial\psi}{\partial s} = \left\{\begin{matrix}(\psi - \psi^{-s})/\Delta s; \mu > 0 \\ (\psi^{+s} - \psi)/\Delta s; \mu < 0\end{matrix}\right\} \tag{7a}$$

$$\frac{\partial}{\partial E}\left(\frac{\psi}{E}\right) = \frac{1}{\Delta E}\left(\frac{\psi^E}{E + \Delta E} - \frac{\psi}{E}\right) \tag{7b}$$

$$\frac{\partial}{\partial E}(\sigma^*\psi) = \frac{1}{\Delta E}[\sigma^*(E + \Delta E)\psi^E - \sigma^*\psi] \tag{7c}$$

$$\begin{aligned}&\frac{\partial}{\partial E}[\sigma^+(E^+ + \langle E\rangle)\psi] \\ &= \frac{\sigma^+(E + \Delta E)\psi^E[E^+ + \langle E\rangle(E + \Delta E)] - \sigma^+\psi(E^+ + \langle E\rangle)}{\Delta E}\end{aligned} \tag{7d}$$

(5) is reduced to

$$\frac{\partial^2\psi}{\partial\theta_0^2} + B\frac{\partial\psi}{\partial\theta_0} - C\psi = D \tag{8}$$

Expressions for the coefficients B, C and D, which are functions of the variables E, θ_0, and s, can be derived using formulas (3), and (7). More details as to how this is done are found in [20], [43]. The functions ψ^{+s} and ψ^{-s} are the values of ψ at the adjacent upper and lower steps in s, ψ^E is the value of ψ at the next higher energy step, and ΔE and Δs are the step lengths in E and s. By Gaussian elimination, (8) is solved.

Test runs show that ten points are sufficient to describe the loss cone. This ensures a reasonable accuracy of the calculation of the plasmaspheric transmittance for electron flux

$$\Pi(E) = \frac{\int_{\mu_{oB}}^1 \mu_o\psi(E,\mu_o,s_1)d\mu_o}{\int_{\mu_{oB}}^1 \mu_o\psi(E,\mu_o,-s_1)d\mu_o} \tag{10}$$

and the relative heating of the electron population

$$C_e(s) = 4\pi A\int_{E_{min}}^{\infty}\frac{\psi_o(E,s)}{E}dE \tag{11}$$

where ψ_o is given by (10a).

To calculate the electron angular distribution at the top of the flux-tube $L = 2$ the number of points in the range $|\mu_{oB}| < |\mu_o| < 1$ is typically 60 for a run considering the energy range 1 eV $< E <$ 50 eV with $\Delta E = 1$ eV.

Modeling collisional interactions between electrons and the neutral atmosphere requires a knowledge of cross-sections of the processes involved. The cross-sections of inelastic collisions of electrons with atoms and molecules were inferred from data reported by [44] and [45]. The cross-sections for collisional ionization were approximated by the expressions given in [11]

$$I_\alpha^+(E,E_2) = \frac{2}{\pi\langle E\rangle_\alpha}\frac{\sigma_\alpha^+(E)}{1+(E_2/E_\alpha)^2} \tag{12}$$

where $\langle E\rangle_\alpha$ are empirical coefficients. Total cross-sections of elastic collisions of electrons with neutral species were specified according to [11], [32], and [46]. More information on the description of collisional interactions in the model is given in the appendix.

A. The Ionosphere and Plasmasphere Decoupled

As mentioned earlier, the photoelectron flux is often estimated for the ionosphere and the plasmasphere separately, by assuming certain boundary conditions at the ionosphere-plasmasphere boundary. This approximation can also be realized in the framework outlined above. In the following we investigate the problems incurred by the separation of the system into two regions, and the results one obtain with this approach.

First we consider photoelectron transport in the mid-latitude magnetosphere. The ionospheric altitude range is excluded from consideration and boundary conditions are imposed at an altitude corresponding to $\pm s_1$:

$$\psi(E,\mu_o,s) = \psi^+(E,\mu_o),\quad s = -s_1,\ \sqrt{1-B_o/B(-s_1)} \le \mu_o \le 1$$
$$\psi(E,\mu_o,s) = \psi^-(E,\mu_o),\quad s = +s_1,\ -1 \le \mu_o \le -\sqrt{1-B_o/B(s_1)}$$

This is a general way of imposing boundary conditions when solving the kinetic equation in a limited region. As an example, we examine the case of an isotropic distribution of electrons with an exponential energy spectrum [34], [43]

$$\psi^+(E,\mu_o) = E\exp(-E/E_o),\quad \sqrt{1-B_o/B(-s_1)} < \mu_o \le 1$$
$$\psi^-(E,\mu_o) = E\exp(-E/E_o),\quad -1 \le \mu_o < -\sqrt{1-B_o/B(s_1)} \tag{13}$$

The question of how to impose boundary conditions it the points $(\mu_o, s) = (\pm\mu_{oB}, \pm s_1)$ remains unclear. This issue is very important because the distribution function imposed at this point largely determines the amount of reflecting flux and therefore the value of the transmittance II. The quantities ψ^+ and ψ^- at $\pm\mu_{oB}$ in essence determine the distribution function on the loss-cone boundary. Physically, the flux at the loss-cone is a result of processes that lead to particle diffusion across the loss-cone boundary. Evidently, the problem is not consistent as stated, and the calculation of key parameters such as II is sensitive to the choice of boundary conditions.

However, with certain assumptions one can solve the kinetic equation. In [36], for instance, a solution was sought for electrons in the loss-cone. In this case, the evolution of the fluxes entering the plasmasphere through each of the ends of the magnetic flux-tube is examined independently. Since the trapped electrons are excluded from consideration, one can use

$$\psi(E,\mu_o,s)|_{\mu_{oB}} = 0. \tag{14}$$

This condition enables one to get rid of the need for iteration processes to determine the flux along μ_{oB}, as discussed later.

Another approximation may be to impose some constant non-zero level of the fluxes

$$\psi^+(\mu_o) = \psi^-(-\mu_o) = \text{ constant},\quad \sqrt{1-B_o/B(\pm s_1)} \le |\mu_o| \le 1 \tag{15}$$

Finally, one may use an iteration scheme to determine ψ^+ and ψ^- at μ_{oB}. Using as a first approximation one of the methods described above, one can find the correct boundary conditions along μ_{oB} by the requirement that the solution for the flux in the positive direction be consistent with the flux along the negative direction of s for $-\mu_{oB}$. The degree of accuracy obtained in this way will be assessed later on the basis of a unified solution for the ionosphere and magnetosphere.

In Fig. 2 are shown the plasmaspheric transmittance for the different ways of imposing the boundary conditions mentioned above. Curve 1 corresponds to the conditions (14), curve 2 to conditions (15), and curves 3 to the iterative method. The results have been obtained for $E_o = 5$ eV at $L = 2$. An increase in E_o up to 10 eV, as shown for the iterative case,

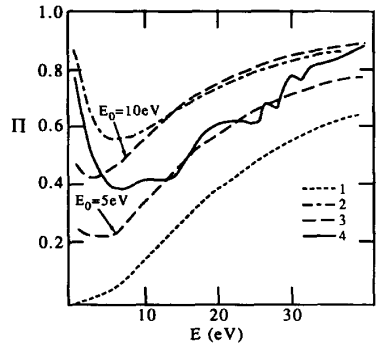

Fig. 2. Models of the plasmaspheric transmittance on $L = 2$ for different ways of imposing the boundary conditions. Curve 1 corresponds to the conditions (14), curve 2 to conditions (15) and curves 3 to the iterative method with $E_o = 5$ and 10 eV. Curve 4 is obtained with ionosphere-plasmasphere transport taken into account jointly.

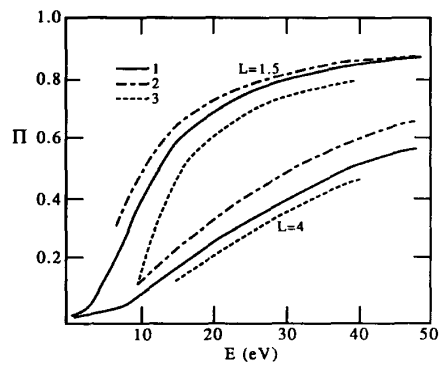

Fig. 3. The plasmaspheric transmittance calculated for two values of L using our own method (curve 1) and compared to the analytical solution [36] (curve 2) and a Monte-Carlo calculation [36] (curve 3). Identical physical assumptions have been used in the three models.

provides some increase in transmittance. This change is due to the first term on the right hand side of equation (3a) of the electron Coulomb collision term, which contains the derivative of the flux with respect to the energy. A comparatively low value of transmittance is found in case 1 because only those electrons that cross the plasmasphere without reversing their direction are counted. For small energies, where the cross-sections of Coulomb scattering are large, the number of such electrons is negligible. Nevertheless, photoelectron fluxes escaping the plasmasphere at these energies must really exist because trapped electrons eventually scatter into the loss cone. Therefore, curves 2 and 3, which have been obtained allowing diffusion into the loss cone, find a finite, non-zero value for the transmittance at low energies. Curve 4 is obtained with ionosphere-plasmasphere transport taken into account jointly, and will be discussed later in the text.

The results discussed above show that the "plasmaspheric" method is sensitive to the boundary conditions introduced between the ionosphere and magnetosphere. To verify that the results presented in Fig. 2 are not influenced by the numerical technique used to solve the equations, we tested the simplest problem (14) against other numerical techniques using the same boundary condition. In Fig. 3 shows our own results for two values of L (curve 1), against an analytical solution [36] (curve 2), and a Monte-Carlo calculation [36] (curve 3). As is evident, the results agree well, which confirms the accuracy of our numerical algorithm.

Till now we have examined a simplified description of photoelectrons in the magnetosphere, namely, the kinetic equation with boundary conditions in the angular and energy distribution of electrons leaving the ionosphere and penetrating into the plasmasphere. It was shown that the predicted value of the transmittance depends substantially on the boundary conditions and on assumptions on the diffusion of electrons across the loss-cone boundary. We now consider the inverse problem: to determine the importance of plasmaspheric transport on the distribution of photoelectron fluxes in the ionosphere. For that purpose we consider the region from 90 km to 1000 km. The problem is reduced to selecting an upper boundary condition for electrons entering the ionosphere from the plasmasphere, i.e., for angles $-1 \leq \mu_o \leq -\sqrt{1 - B_o/B(s_1)}$.

The problem has been studied in two limits. The first assumes absolute transparency of the plasmasphere, in other words, that plasmaspheric transport of photoelectrons bears a collisionless character. For symmetric conditions of illumination the the boundary condition is

$$\psi(E, \mu_o, s_1) = \psi(E, -\mu_o, s_1), \sqrt{1 - B_o/B(s_1)} \leq \mu_o \leq 1 \tag{16}$$

where s_1 again corresponds to the boundary between the ionosphere and plasmasphere.

In the second limit it is assumed that the plasmasphere is absolutely non-transparent and that no flux enters the ionosphere at the upper boundary

$$\psi(E, \mu_o, s_1) = 0, \sqrt{1 - B_o/B(s_1)} \leq \mu_o \leq 1 \tag{17}$$

Fig. 4 shows the omnidirectional flux of photoelectrons at 830 km altitude. Curve 1 corresponds to collisionless plasmaspheric transport ($\Pi = 1$), curve 2 to the non-transparent case ($\Pi = 0$), and curve 3 to our unified approach that considers the ionosphere and magnetosphere jointly. In this case, symmetric illumination of the hemispheres has been assumed. The last variant will be discussed more later, at this point it may be used to assess the accuracy of the two limits for the boundary conditions. From the figure it can be seen that a unified, self-consistent treatment gives values that are in-between the two limits (16) and (17) as expected. The assumption $\Pi = 1$ on $L = 2$ is seen to be more accurate at the higher energies (30–40 eV) overestimating the flux levels by 10–15%, while at lower energies (<10 eV) the error has increased to 80–100%. At higher L-shells this error affects an increasing range of energies. At $L = 4$, for instance, the flux below about 20 eV is significantly overestimated. The case $\Pi = 0$ leads to significant underestimation throughout the entire energy range.

Again, the numerical algorithm has been tested against the results of other methods in order to assess its accuracy. For this purpose, discrete energy loss has been assumed ((6a) and (7a)) rather than the continuous energy loss approximations ((8a) and (9a)). The case of $\Pi = 0$ was chosen such that

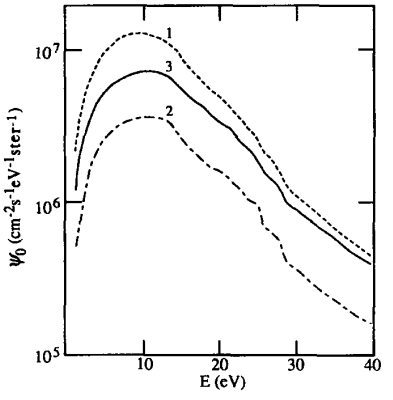

Fig. 4. Model calculations of differential energy flux of electrons on $L = 2$ at 830 km altitude. (1) $\Pi = 1$, (2) $\Pi = 0$ and (3) our unified model.

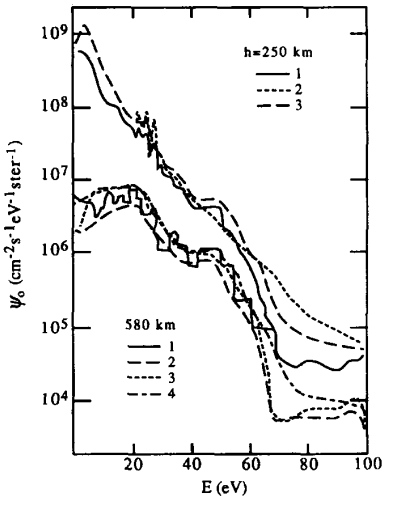

Fig. 5. Comparison of omnidirectional differential energy flux of electrons. On the upper part of the plot are shown spectra at 250 km altitude. Curve 1 is from [48], curve 2 is an experimental observation [30] and curve 3 is our own calculation. On the lower portion of the plot are shown spectra at 580 km altitude. Curve 1 is from [28], [49], curve 2 from [4], [32], curve 3 from [50], [51], and curve 4 our own calculation.

the assumptions used in the model, including the values of the cross-sections, neutral densities etc., are identical to the ones used in the models we compare against. Results for the omnidirectional flux are shown in Fig. 5. On the upper part of the plot are shown spectra at 250 km altitude. Curve 1 is from [48], curve 2 is an experimental observation [30], and curve 3 is our own calculation. On the lower portion of the plot are shown spectra at 580 km altitude. Curve 1 is from [28], [49], curve 2 from [4], [32], curve 3 from [50], [51], and curve 4 our own calculation. Fig. 6 shows energetic atmospheric photoelectrons at 172.5° pitch angle (upward flux) and 590 km altitude observed by the low altitude plasma instrument on Dynamics Explorer 2 (curve 1) [52] against theoretical calculations using [13] (curve 2), [32] (curve 3), and our own model (curve 4). All models include K-shell ionization effects and predict peaks in the photoelectron spectrum due to Auger electrons emitted from oxygen and nitrogen. All theoretical calculations were performed for the same conditions which were discussed by [52]. As can be seen, the results are in very good agreement, which confirms a good accuracy of our numerical algorithm.

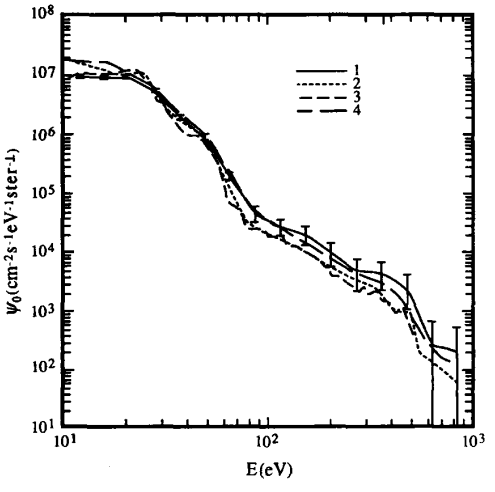

Fig. 6. Comparison of energetic atmospheric photoelectron fluxes. The flux at 172.5° pitch angle (upward flux) and 590 km altitude observed by the low altitude plasma instrument on Dynamics Explorer 2 [52] (curve 1) and theoretical calculations using [13] (curve 2), [32] (curve 3) and the unified model (curve 4). The theoretical calculations were performed for the same conditions discussed in [52].

B. The Ionosphere and Plasmasphere Unified

Results obtained by solving the kinetic equation (3) in the ionosphere and plasmasphere simultaneously have already been presented in Figs. 2 and 4 (solid curves). They will now be discussed in more detail.

By studying the ionosphere and plasmasphere as one system rather than two separate ones, substantial corrections are introduced in the values and characteristics of key parameters describing photoelectron fluxes. This is most clearly exemplified in the concept of the plasmaspheric transparency. The fact that processes are included such as diffusion across the loss-cone boundary, reflection in the ionosphere due to elastic collisions with neutral and charged particles, and the redistribution of the flux at low energies due to interactions with neutral and charged particles, makes the term "transparency" acquire its conventional meaning (10).

In Fig. 2, the transparency Π is shown as a function of energy. As mentioned earlier, curve 4 corresponds to the case with the ionosphere and plasmasphere taken into account jointly, while curves 1–3 represent models treating the plasmasphere as a separate region. First of all, note that Π as shown by curve 4 has considerable structure. This feature is a result of the structure in the flux created by photoionization (the source) and by collisional interactions between suprathermal electrons and neutral particles in the ionosphere. As this flux propagates through the plasmasphere, particles undergo Coulomb collisions at a rate dependent on $\partial\psi/\partial E$ as seen from (3a), and thus some structure is induced

in the transparancy. Note that the structure of the suprathermal electron flux obtained in our calculations does not contain the complete fine structure of the ionospheric spectrum because of our use of the continuous energy-loss approximation for electron-neutral collisions. The finite value of Π at small energies is caused primarily by a contribution from the trapped electron population, which has diffused down to low energies and subsequently into the loss-cone, thereby increasing the value of the transparency. It is clear that in this case Π characterizes diffusion from the trapped region into the loss-cone, rather than the transmitting capability of the flux-tube.

The increase of Π with decreasing energy seen below $\simeq 8$ eV is caused by the formation of a plateau-like part of the photoelectron distribution function in the upper ionosphere and plasmasphere. The Coulomb collision term (3a) is small in this situation because it contains the term $\partial f/\partial E$. The exact shape of the function at low energies, and therefore the location of the minimum in Π, depend on the integrated content of thermal particles in the flux-tube [53].

The physical interpretation of Π is not always clear. Some insight can be gained by defining a simpler parameter, namely the integrated transparency. Following the terminology of [34], it can be defined as the ratio of the number of particles leaving one end of a magnetic flux-tube to the number of particles entering at the other end

$$T = P_2/P_1. \tag{18}$$

The flux on the boundaries of the plasmasphere is made up of three contributions: 1) newly produced photoelectrons arriving from their regions of production, 2) electrons reflected in the conjugate ionosphere, and 3) electrons diffusing into the loss-cone from the trapped region.

To describe these contributions qualitatively we introduce the following quantities: α, the probability that an electron will cross the plasmasphere staying inside the loss-cone (the probability of diffusion across the loss-cone boundary into the trapped region is then $1-\alpha$), 2 β, the probability that a trapped electron scatters into the loss cone and is lost before it has been thermalized, and A_1 and A_2, the probabilities of reflection in the conjugate ionosphere (albedo). We shall assume that the thermal plasma density is distributed symmetrically along the geomagnetic field with respect to the top of the field line. Then the probability of diffusion into the loss cone and arriving at either end of the flux-tube will be the same and equal to β.

We now examine the general case with arbitrary illumination of the two hemispheres, and electron fluxes P_{01} and P_{02}, generated by local photoionization, entering the plasmasphere from the two ends of the flux-tube. If we take into account multiple reflection of electrons in conjugate regions, the flux entering the plasmasphere from region 1 is

$$(P_{01} + P_{02}\alpha A_1)(1 + \alpha^2 A_1 A_2 + \alpha^4 A_1^2 A_2^2 + \cdots) \equiv \frac{P_{01} + P_{02}\alpha A_1}{1 - \alpha^2 A_1 A_2}$$

A similar result is found for region 2 by switching the subscripts 01 and 02, and 1 and 2. The sum of these fluxes multiplied by the probability of trapping, will give the number of electrons entering the trapping zone. Electrons diffusing back into the loss-cone from the trapping zone and subsequently reflecting in the ionosphere will cause the existence of additional fluxes entering into the plasmasphere from the two conjugate regions, equal to

$$[P_{01}(1 + \alpha A_2) + P_{02}(1 + \alpha A_1)] \times (1 - \alpha)\beta A_1(1 + \alpha A_2)/(1 - \alpha^2 A_1 A_2)^2$$

and

$$[P_{01}(1 + \alpha A_2) + P_{02}(1 + \alpha A_1)] (1 - \alpha)\beta A_2(1 + \alpha A_2)/(1 - \alpha^2 A_1 A_2)^2.$$

Continuing this iteration process one obtains expressions for the total electron fluxes at the plasmaspheric boundaries in the form of a diminishing series. The total number of particles entering into the plasmasphere from the region 1 is found to be

$$P_1 = \frac{P_{01} + P_{02}\alpha A_1}{1 - \alpha^2 A_1 A_2} + \frac{[P_{01}(1 + \alpha A_2) + P_{02}(1 + \alpha A_1)](1 - \alpha)\beta A_1(1 + \alpha A_2)}{(1 - \alpha^2 A_1 A_2)\{1 - \alpha^2 A_1 A_2 - (1 - \alpha)\beta[A_1(1 + \alpha A_2) + A_2(1 + \alpha A_1)]\}} \tag{19}$$

while the number of particles leaving the plasmasphere into the region 2 is

$$P_2 = \alpha P_1 + \frac{[P_{01}(1 + \alpha A_2) + P_{02}(1 + \alpha A_1)](1 - \alpha)\beta}{\{1 - \alpha^2 A_1 A_2 - (1 - \alpha)\beta[A_1(1 + \alpha A_2) + A_2(1 + \alpha A_1)]\}} \tag{20}$$

Using (19) and (20) we can now derive an expression for integrated transparency T in accordance with the definition (18).

Consider now the following cases: (1) $\beta = 0$: Here it is assumed that electrons, after being trapped, are incapable of again entering the loss cone. In this case $T = \alpha$, and the transparency is independent of the character of illumination and the albedo of the ionosphere. In this case, the plasmasphere can be studied separately from the ionosphere and the probability α can be calculated as a function of the integrated content of thermal particles in the flux-tube [53]. (2) $P_{01} = P_{02}, A_1 = A_2$: In this case the conjugate hemispheres are illuminated symmetrically and $T = \alpha + 2(1 - \alpha)\beta$. Here T is independent of A_1 and A_2. Since the conditions are symmetric, the value of T is the same whether calculated referenced to one end of the flux-tube or the other end. Our result that $T \leq 1$ is at first glance in contradiction with the fact that we are investigating the time-stationary equation, because it means that more suprathermal electrons enter the flux-tube than leave the flux-tube. The sink of suprathermal electrons that assures that the particle distribution is constant in time is provided by the diffusion of particles through the lower energy boundary of the suprathermal regime and into the thermal particle population.

An analysis of the general case shows that T is a function of both the illumination and the reflectivity of the ionospheric, with T decreasing as the asymmetry of the conditions increases. This dependency can be understood from the following argument. In the symmetrical case the trapping zone

becomes filled with electrons produced in the two conjugate regions. These electrons are then scattered into the loss-cone and lost at the two ends of the flux-tube. In the asymmetric case, the trapping zone is filled mainly by electrons from the one illuminated region, but electrons are still lost in both hemispheres. In the latter case, however, the back-scatter in the ionosphere is a symmetrizing factor because the reflection in the non-illuminated region produces an effective source of electrons.

It is now possible to make some conclusions regarding the differential transparency. The largest dependence with geophysical conditions is expected for small energies where pitch-angle diffusion is the strongest. An increase in electron energy is accompanied by an increase in $\alpha(E)$ and a decrease in $\beta(E)$, i.e., $T(E) \simeq \alpha(E)$ and less dependent on geophysical conditions. These conclusions agree with the numerical calculations of the differential transparency $\Pi(E)$ shown in Fig. 7 and the analytical solution of [53]. In Fig. 7, $\Pi(E)$ is calculated under three geophysical conditions: symmetric illumination of conjugate regions (curve 1), photoelectron source in one hemisphere only (curve 2), and for elastic scattering of photoelectrons by neutral particles of the dark hemisphere region "switched off" (curve 3). As can be seen in Fig. 7, the differential transparency has a tendency to decrease with increasing asymmetry of ionospheric conditions, in particular for the lower energies. Note, that the variations in Π with ambient conditions is not a reflection of changes in the number of electrons penetrating into the plasmasphere, i.e., changes in the magnitude of ψ shown in the lower portion of the figure, because the underlying equations are linear. Rather, it is dependent on the asymmetric conditions, or the relative contribution, of the conjugate ionospheres. It is worth pointing out that a similar analysis cannot be applied to methods that consider the plasmasphere isolated from the ionosphere.

Fig. 8 shows one of the applications of the model: the calculation of the heating of thermal electrons. Curve 1 corresponds to symmetric illumination calculated along $L = 2$, curve 2 to heating in the sunlit ionosphere with darkness in the conjugate ionosphere, and curve 3 to heating in the dark ionosphere. Also shown is the electron density profile used in the calculation. It is seen that without the photoelectron source in one of the ionospheres, the heating decreases by a factor 2 (curve 2).

A method sometimes used to describe photoelectrons along a closed field line simplifies effects of inhomogeneities in the magnetic field by averaging the kinetic equation over bounces between opposite hemispheres. To do this, the distribution function is assumed constant along the characteristics of motion [41]. The validity of this approximation can be evaluated from our unified model by comparing the solution $\psi(\mu_o, s)$ at the boundary of the plasmasphere ($s = -s_1$) and at the top of the field line ($s = 0$) at a constant value of μ_o. Fig. 9 shows the ratio of these values at $\mu_o = \mu_{oB}$ as a function of energy and electron content of the flux-tube $L = 2$. Curve 1 corresponds to the profile depicted in Fig. 8, while curves 2 and 3 are obtained for densities two and four times larger. It is clear that the flux is not constant below energies of $\sim$ 10 eV and that for higher densities, the flux increasingly varies along the field line. Only at energies above $\sim$ 10 eV (approximately equal to the

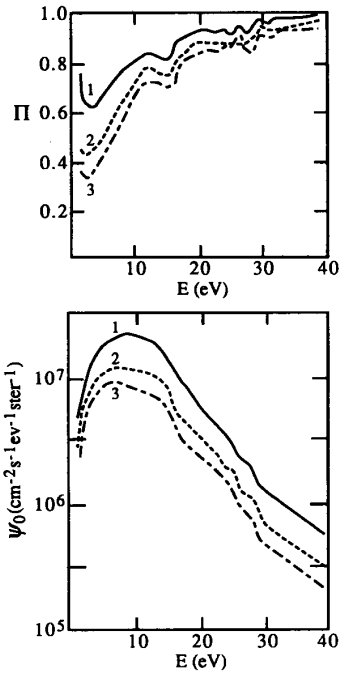

Fig. 7. The transparency Π (top panel) and the differential energy flux of electrons on $L = 2$ for: (1) symmetric illumination of the conjugate hemispheres, (2) one hemisphere illuminated only and (3) one hemisphere illuminated and no elastic scattering in the dark hemisphere.

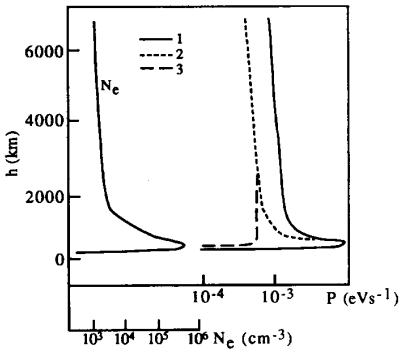

Fig. 8. Heating of the thermal electron population on $L = 2$. (1) both hemispheres illuminated, (2) heating in the illuminated hemisphere, the conjugate dark and (3) heating in the dark hemisphere.

mean energy of photoelectrons in the plasmasphere) is the flux relatively constant and thus the method of bounce averaging valid. The plasmaspheric transparency estimated under four assumptions was discussed earlier (Fig. 2). It is now clear why there is a drastic discrepancy between our inclusive model (curve 4), and the model with boundary conditions imposed at the topside ionosphere and corrected through an iterative procedure (curve 3). In the latter case, the correction has been done using the bounce averaging technique. The inaccuracy of this technique at low energies explains the discrepancy seen in particular below 10 eV. Again, this value is calculated for

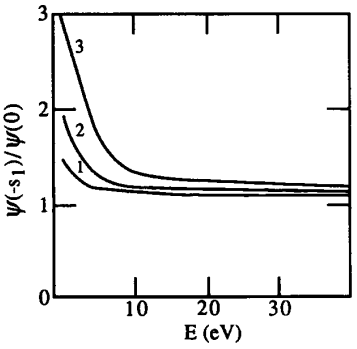

Fig. 9. Variation of $\psi(\mu_{oB}, s)$ with s and E. Curve 1 corresponds to the density profile depicted in Fig. 8, while curves 2 and 3 are obtained for densities two and four times larger.

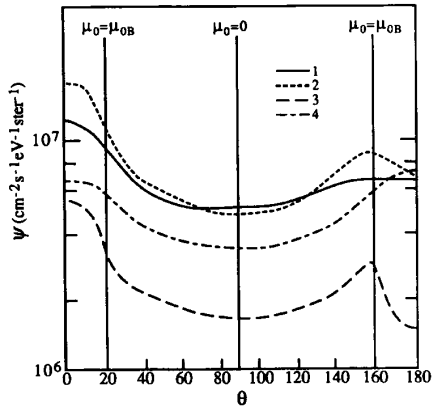

Fig. 10. Pitch-angle distributions of photoelectrons at the magnetic equator on $L = 2$ using the unified model. Curves 1–3 are for the asymmetric case ofphotoionization in one hemisphere for electrons at 5, 10 and 20 eV. The distribution calculated in the case of symmetric illumination for 20 eV-electrons (curve 4) is shown for comparison. The electron density profile used is the same as the one shown in Fig. 8.

$L = 2$. At higher L-shells, the error is significant below $\simeq$ 15 eV.

Fig. 10 shows the pitch-angle distribution of photoelectrons at the apex of the field line $L = 2$ using the unified model. Curves 1–3 are for the asymmetric case of photoionization in one hemisphere for electrons at 5, 10, and 20 eV. The distribution calculated in the case of symmetric illumination for 20 eV-electrons (curve 4) is shown for comparison. The electron density profile used is the same as the one shown in Fig. 8. It is of interest that despite the extreme asymmetry of the conditions, the angular distribution in the trapped zone is almost symmetric, which reflects the "mixing" of trapped electrons through bounces in the magnetosphere. Some isotropization is also effective at the lower energies due to the enhanced diffusion across the loss-cone boundary at these energies.

IV. Discussion

We have presented a kinetic description of suprathermal electrons in the Earth's ionosphere and plasmasphere. The model has been applied to the problem of photoelectron fluxes in the mid-latitude magnetosphere. We also applied the model to the various limits for which methods were developed in the past. This allowed us to discuss the validity of the assumptions used in these methods, and to address much of the basic physics of suprathermal electrons. Some of the main conclusions are outlined below.

For the plasmasphere, our approach allows the study of the ionosphere and the plasmasphere as one system, without dividing them into two separate regions. This "unified" approach avoids difficulties of specifying the boundary conditions at the ionosphere-plasmasphere boundary. We have demonstrated that in almost all aspects of photoelectron dynamics, important features are lost when treating the two regions separately, in particular for electrons at energies below 10–20 eV. Since this energy is close to the median photoelectron energy, the errors introduced by the separate treatment of the regions can be quite significant.

When attempting to study the magnetosphere separately from the ionosphere, the problem of specifying a boundary condition at the top-side ionosphere is exacerbated by the fact that this boundary also introduces an artificial boundary between loss-cone and trapped particle fluxes. The loss-cone is defined by this altitude, because fluxes that leave the plasmasphere and enter the ionosphere are lost and therefore are in the loss-cone. Thus, the flux specified at the topside ionosphere boundary at 90° pitch-angle to a large extent determines the flux at the loss-cone boundary along the complete field-line. This is unfortunate, because it is in the diffusion of particles across the loss-cone boundary that much of the important physics is located.

The kinetic description of the plasmaspheric suprathermal population does not include wave-particle interactions. It is known that plasma waves are important in the dynamics of the plasmasphere, providing a means for transfer of energy between different particle populations and diffusion of electrons across the loss-cone boundary and into the upper atmosphere. The inclusion of wave-particle interactions will be an important next step in the further development of the model.

Appendix

A. Coulomb Collisions

When describing Coulomb interactions of electrons with charged particles, the Landau collision integral is often used, but on a linearized form, assuming that the thermal electrons and ions can be described by Maxwellian distribution functions [55]

$$\langle S_{ee}\rangle = An_e\left\{\frac{\partial}{\partial E}\left[\frac{\psi}{E}+T_e\frac{\partial}{\partial E}\left(\frac{\psi}{E}\right)\right]+\frac{1}{4E^2}\frac{\partial}{\partial\mu}\left[(1-\mu^2)\frac{\partial\psi}{\partial\mu}\right]\right\} \quad (1a)$$

$$\langle S_{ei}\rangle = An_i\left\{\frac{m_e}{m_i}\frac{\partial}{\partial E}\left[\frac{\psi}{E}+T_i\frac{\partial}{\partial E}\left(\frac{\psi}{E}\right)\right]+\frac{1}{4E^2}\frac{\partial}{\partial\mu}\left[(1-\mu^2)\frac{\partial\psi}{\partial\mu}\right]\right\} \quad (2a)$$

where $A = 2\pi e^4 \ln L = 2.6 \times 10^{-12}$ eV^{2}cm^2, and $\ln L$ is the Coulomb logarithm. Further, one can show that the term $\partial^2(\psi/E)/\partial E^2$ is small compared to the other terms in (1a) [9]. Neglecting this derivative and the energy loss in collisions with ions ($m_e/m_i \ll 1$) in (2a), (1a) and (2a) becomes

$$\langle S_{ee}\rangle + \langle S_{ei}\rangle = An_e\left\{\frac{\partial}{\partial E}\left(\frac{\psi}{E}\right) + \frac{1}{2E^2}\frac{\partial}{\partial \mu}\left[(1-\mu^2)\frac{\partial \psi}{\partial \mu}\right]\right\} \tag{3a}$$

where n_e is the density of the thermal electrons. Arriving at (3a), the condition of plasma quasi-neutrality ($n_e = n_i$) has been used.

B. Elastic Collisions

The term describing elastic collisions of electrons with neutral particles is [56]

$$\langle S_{e\alpha}\rangle = 2\frac{m_e}{m_\alpha}n_\alpha\frac{\partial}{\partial E}\left\{\sigma_\alpha^{(1)}E^2\left[\frac{\psi}{E} + T_n\frac{\partial}{\partial E}\left(\frac{\psi}{E}\right)\right]\right\} + n_\alpha\int I_\alpha(E,\chi)[\psi(E,\mu') - \psi(E,\mu)]\,d\Omega \tag{4a}$$

where the scattering ($\mu' \to \mu$) is described by the scattering angles (χ, η), with $\mu' = \cos\chi\cos\theta + \sin\theta\sin\chi\cos\eta$ and the solid angle $d\Omega = \sin\chi d\chi d\eta$. The density of neutral particles of species α is n_α, the transport cross-section is $\sigma_\alpha^{(1)}(E) = \int I_\alpha(E,\chi)(1-\cos\chi)d\Omega$, and the differential elastic cross-section is $I_\alpha(E,\chi)d\Omega$.

A convenient approximation of (4a) is

$$\langle S_{e\alpha}\rangle = \frac{n_\alpha\sigma_\alpha^{(1)}}{2}\frac{\partial}{\partial\mu}\left[(1-\mu^2)\frac{\partial\psi}{\partial\mu}\right] \tag{5a}$$

Strictly speaking, (5a) is physically justified only for high-energy electrons when the interaction with the Coulomb field of a scattering center is of primary importance. Nonetheless, we found that when solving the kinetic equation, the replacement of the isotropic type of elastic scattering (4a) by the Coulomb one (5a) does not result in great differences in the determination of the flux at energies $E > 1$ eV. [8] showed that the error caused by the replacement of isotropic scattering with forward peak scattering of incident electrons with energies of a few tens eV constitutes 20%–30%. It should be emphasized that forward peak scattering leads to an increase of the secondary electron production rate, which to some extent compensates for the underestimation of the flux when the approximation of continual energy loss is applied as shown below. Thus, expression (5a) may be used when solving (1) throughout the complete energy range of interest. We note at this point, that the introduction of (5a) is not necessary for solving the kinetic equation. It is introduced only to increase the speed of the computational algorithm.

C. Inelastic Collisions

Expressions describing inelastic collisions with neutral particles are also derived using a number of well-known approximations. Let us assume that the dissipating electron does not change direction (is forward scattered) and, if ionization occurs, that the secondary electron is emitted perpendicular to the velocity of the initial electron before the collision [57]. Then $\langle S_{e\alpha}^*\rangle$ and $\langle S_{e\alpha}^+\rangle$ can be written on the form [48]

$$\langle S_{e\alpha}^*\rangle = n_\alpha\sum_j[\sigma_{\alpha j}^*(E+E_{\alpha j}^*)\psi(E+E_{\alpha j}^*,\mu) - \sigma_{\alpha j}^*(E)\psi(E,\mu)] \tag{6a}$$

$$\langle S_{e\alpha}^+\rangle = n_\alpha\int_{E+E_\alpha^+}^{2E+E_\alpha^+} I_\alpha^+(E', E'-E-E_\alpha^+)\psi(E',\mu)dE' + \frac{n_\alpha}{2\pi}\int_{2E+E_\alpha^+}^{\infty} I_2^+(E',E)\int_0^{2\pi}\psi(E',\sqrt{1-\mu^2}\cos\eta)d\eta dE' - n_\alpha\sigma_\alpha^+(E)\psi(E,\mu) \tag{7a}$$

where $\sigma_{\alpha j}^*$ is the total cross-section of scattering bringing a neutral particle into an excited state characterized by a threshold energy $E_{\alpha j}^*$, and the ionization energy is E_α^+. We also have

$$\sigma_\alpha^+ = \int_0^{(E-E_\alpha^+)/2} I_\alpha^+(E,E_2)dE_2$$

which is the total cross-section of ionization by an electron with energy E. $I_\alpha^+(E,E_2)$ is the appropriate differential cross-section, and E_2 is the energy of a secondary electron.

To further simplify (6a) and (7a) we use the continuous energy loss approximation [58]. This approximation is valid for high energy electrons, for which the energy lost during a collision is small in comparison with the original electron energy. Although this condition is not always fulfilled for suprathermal electrons, there is some experience of successfully using the continuous loss approximation at certain energy ranges, when calculating photoelectron spectra in the ionosphere [43]. Problems are encountered only in regions with a pronounced fine structure of the energy spectrum, in particular near the photo ionization peaks at $E = 22$–27 eV.

Using a Taylor series expansion of functions with argument on the form $E + dE$, (6a) and (7a) become

$$\langle S_{e\alpha}^*\rangle = n_\alpha\sum_j E_{\alpha j}^*\frac{\partial}{\partial E}[\sigma_{\alpha j}^*(E)\psi(E,\mu,s)] \tag{8a}$$

$$\langle S_{e\alpha}^+\rangle = n_\alpha\left\{\frac{\partial}{\partial E}[\sigma_\alpha^+(E)\psi(E,\mu,s)(E_\alpha^+ + \langle E\rangle_\alpha)] + \int_{2E+E_\alpha^+}^{\infty} I_\alpha^+(E',E)\psi_0(E',s)dE'\right\} \tag{9a}$$

where

$$\langle E\rangle_\alpha = \frac{1}{\sigma_\alpha^+}\int_0^{(E-E_\alpha^+)/2} E_2 I_\alpha^+(E,E_2)dE_2$$

is the average energy of secondary electrons. The second term on the right-hand side of (9a) defines the electron production rate due to collisional ionization of atmospheric species assuming the distribution function is isotropic

$$\psi_0(E,s) = \frac{1}{2}\int_{-1}^{1}\psi(E,\mu,s)d\mu \tag{10a}$$

Let us evaluate the accuracy of the approximation of continuous loss (8a–9a) in the low-energy region, where a major

part is played by secondary electrons. The approximation is based on the two first terms in the expansion:

$$\xi(E + \langle E^* \rangle) = \sum_{n=0}^{\infty} \frac{\langle E^{*n} \rangle}{n!} \frac{\partial^n \xi}{\partial E^n}.$$

Here $\xi = \langle \sigma \rangle \psi$, and $\langle \sigma \rangle$ and $\langle E^* \rangle$ are some effective values of the inelastic scattering cross-section and energy loss. Noting that ξ, in the local approximation, is defined by the energy spectrum of the electron production source, the uncertainty introduced by the approximation of continuous loss must be of the order of

$$\epsilon = \frac{\langle E^* \rangle}{2E_o} \tag{11a}$$

where E_o is the characteristic energy of the secondary electron production spectrum. Both E^* and E_o decrease with decreasing E, while ϵ nowhere exceeds 30%.

A more accurate evaluation of the error introduced by assuming continuous energy loss can be found by comparison to electron spectra calculated without this assumption. This was done for the case of photoelectrons in the lower and upper ionosphere [14]. It was concluded that significant error was introduced only in the range from 22–27 eV, where the electron spectrum is sharply peaked due to ionization of the atmosphere by solar radiation [42]. However, the secondary electron spectrum, produced by impact ionization, does not have these peaks, which decreases the significance of the total error introduced. The sharp minimum in the electron distribution often observed at $E < 4$ does not affect the accuracy of the approximation because it is caused by the large value of the cross-section of oscillatory excitation of molecular nitrogen, rather than by a non-monotonicity in the energy spectrum of production. The resulting $\xi(E)$ function, therefore, is a fairly smooth one.

Again we point out that the assumption of continuous energy loss over the whole energy range is not a necessity, but a convenient way of reducing the complexity of the numerical algorithm. Calculations showing the fine structure at the low-energy portion of the suprathermal spectrum using (6a–7a) have been presented in [14].

The terms $\langle S^*_{\alpha i} \rangle$ and $\langle S^-_{\mathrm{ei}} \rangle$ can generally be neglected because of the prevalence of neutral particles over ions as well as the small value of the cross-section of dissociative recombination for suprathermal electrons.

REFERENCES

[1] G. A. Victor, K. Kirby-Docken and A. Delgarno, "Calculations of the equilibrium photoelectron flux in the thermosphere," *Planet. Space Sci.*, vol. 24, p. 679, 1976.

[2] J. R. Jasperse, "Boltzmann-Fokker-Planck model for the electron distribution function in the earth's ionosphere," *Planet. Space Sci.*, vol. 24, p. 33, 1976.

[3] J. R. Jasperse, "Electron distribution function and ion concentrations in the earth's lower ionsphere from Boltzmann-Fokker-Planck theory," *Planet. Space Sci.*, vol. 25, p. 743, 1977.

[4] P. M. Banks and A. F. Nagy, "Concerning the influence of elastic scattering upon photoelectron transport and escape," *J. Geophys. Res.*, vol. 75, p. 1902, 1970.

[5] G. P. Mantas and S. A. Bowhill, "Calculated photoelectron pitch-angle and energy spectra," *Planet. Space Sci.*, vol. 23, p. 355, 1975.

[6] E. O. Oran and D. J. Strickland, "Calculation of the ionospheric photoelectron distribution function," *Planet. Space Sci.*, vol. 26, p. 1161, 1978.

[7] M. J. Prather, M. B. McElroy and J. Rodriguez, "Photoelectrons in the upper atmosphere: A formulation incorporating effects of transport," *Planet. Space Sci.*, vol. 26, p. 131, 1978.

[8] J. Lejeune, "Two stream photoelectron distributions with interhemispheric coupling: a mixing of analytical and numerical methods," *Planet. Space Sci.*, vol. 27, p. 561, 1979*a*.

[9] G. V. Khazanov and G. D. Gefan, "The kinetics of ionosphere-plasmasphere transport of suprathermal electrons," *Phys. Solarterr., Potsdam*, vol. 19, p. 65, 1982.

[10] R. Link, "Feautrier solution of the electron transport equation," *J. Geophys. Res.*, vol. 97, p. 159, 1992.

[11] P. M. Banks, C. R. Chappell and A. F. Nagy, "A new model for the interaction of auroral electrons with the atmosphere: spectral degradation, backscatter, optical emission and ionization," *J. Geophys. Res.*, vol. 79, p. 1459, 1974.

[12] G. P. Mantas, H. C. Carlson and V. B. Wickwar, "Photoelectron flux buildup in the plasmasphere," *J. Geophys. Res.*, vol. 83, p. 1, 1978.

[13] D. J. Strickland, D. L. Book, T. P. Coffey and J. A. Fedder, "Transport equation techniques for the deposition of auroral electrons," *J. Geophys. Res.*, vol. 81, p. 2755, 1976.

[14] V. M. Polyakov, G. V. Khazanov and M. A. Koen, "Mathematical model of photoelectron fluxes in the mid-latitide ionosphere," *Cosmic Res.*, vol. 14, p. 543, 1976.

[15] K. Stamnes, "Analytic approach to auroral electron transport and energy degradation," *Planet. Space Sci.*, vol. 28, p. 427, 1980.

[16] K. Stamnes, "On the tro-stream approach to electron transport and thermalization," *J. Geophys. Res.*, vol. 86, p. 2405, 1981.

[17] D. J. Strickland, J. R. Jasperse and J. A. Whalen, "Dependence of auroral FUV emission on the incident electron spectrum and neutral atmosphere," *J. Geophys. Res.*, vol. 88, p. 8051, 1983.

[18] S. S. Prasad, D. J. Strickland and Y. T. Chiu, "Auroral electron interaction with the atmosphere in the presence of a conjugated field-aligned electrostatic potential," *J. Geophys. Res.*, vol. 88, p. 4123, 1982.

[19] S. S. Prasad, D. J. Strickland and Y. T. Chiu, "Precipitating electron interaction with the atmosphere 2: The dayside cusp region," *J. Geophys. Res.*, vol. 90, p. 11025, 1985.

[20] G. D. Gefan, A. A. Trukhan and G. V. Khazanov, "A method of calculating auroral electron fluxes," *Ann. Geophys.*, vol. 3, p. 135, 1985.

[21] H. S. Porter, F. Varosi and H. G. Hayr, "Iterative solution of the multistream electron transport equation, 1, Comparison with laboratory beam injection experiments," *J. Geophys. Res.*, vol. 92, p. 5933, 1987.

[22] D. Lummerzheim, M. H. Rees and H. R. Anderson, "Angular dependent transport of auroral electrons in the upper atmosphere," *Planet. Space Sci.*, vol. 37, p. 109, 1989.

[23] P. G. Richards and D. G. Torr, "Aurral modeling of the 3371 Å emission rate: dependance on characteristic electron energy," *J. Geophys. Res.*, vol. 95, p. 10337, 1990.

[24] M. H. Rees, "Auroral energy deposition rate," *Planet. Space Sci.*, vol. 40, p. 299, 1992.

[25] M. J. Berger, S. M. Seltzer and K. Maeda, "Some new results on electron transport in the atmosphere," *J. Atmos. Terr. Phys.*, vol. 36, p. 591, 1974.

[26] M. J. Berger, S. M. Seltzer and K. Maeda, "Energy deposition by auroral electrons in the atmosphere," *J. Atmos. Terr. Phys.*, vol. 32, p. 1015, 1970.

[27] S. C. Solomon, "Auroral electron transport using Monte-Carlo methods," *Geophys. Res. Lett.*, vol. 20, p. 185, 1993.

[28] R. J. Cicerone and S. A. Bowhill, "Photoelectron flux in the ionosphere computed by a Monte-Carlo method," *J. Geophys. Res.*, vol. 76, p. 8299, 1971.

[29] E. G. Fontheim, A. E. Beutler and A. F. Nagy, "Theoretical calculations of the conjugate predawn effects," *Ann. Geophys.*, vol. 24, p. 489, 1968.

[30] Yu. I. Galperin and T. M. Mulyarchik, "On the height distribution of photoelectrons," *Cosmic Res.*, vol. 4, p. 932, 1966.

[31] S. Sanatani and W. B. Hanson, "Plasma temperatures in the magnetosphere," *J. Geophys. Res.*, vol. 75, p. 769, 1970.

[32] A. F. Nagy and P. M. Banks, "Photoelectron fluxes in the ionosphere," *J. Geophys. Res.*, vol. 75, p. 6260, 1970.

[33] T. Takahashi, "Energy degradation and transport of photoelectrons escaping from the upper ionosphere," *Rep. Ionos. Space. Res. Japan.*, vol. 27, p. 79, 1974*a*.

[34] G. Lejeune and F. Wormser, "Diffusion of photoelectron flux in the plasmasphere," *J. Geophys. Res.*, vol. 81, p. 2900, 1976.

[35] G. V. Khazanov, M. A. Koen and S. I. Barayshuk, "Trapped electrons and secondary electrons in the midlatitude plasmasphere 1 & 2," *Cosmic Res.*, vol. 15, no. 68, p. 379, 1977.

[36] I. A. Krinberg and G. K. Matafonov, "Coulomb collision-induced photoelectron trapping by the geomagnetic field and electron gas heating in the plasmasphere," *Ann. Geophys.*, vol. 34, p. 89, 1978.
[37] G. V. Khazanov, M. A. Koen and S. I. Burenkov, "Analysis of plasmaspheric passage of suprathermal electrons," *Phys. Splariterr.*, vol. 15, p. 91, 1981.
[38] G. V. Popov and G. V. Khazanov, "The solution of the kinetic equation for ionospheric photoelectrons with regard to both conjugate regions," *Kosm. Issledovaniya*, vol. 12, p. 241, 1974.
[39] G. P. Mantas, H. C. Carlson and V. B. Wickwar, "Photoelectron flux buildup in the plasmasphere," *J. Geophys. Res.*, vol. 83, p. 1, 1978.
[40] J. Lejeune, "Diffusion of monoenergetic photoelectron fluxes in the plasmasphere," *J. Geophys. Res.*, vol. 84, p. 1481, 1979*b*.
[41] V. M. Polyakov, G. V. Khazanov and M. A. Koen, "The ionosphere-plasmasphere photoelectron transport," *Phys. Solariterr.*, vol. 10, p. 93, 1979.
[42] I. A. Krinberg, L. A. Garifullina and L. A. Akatova, "Photoelectron fluxes and electron gas heating at the lower ionosphere," *J. Atmos. Terr. Phys.*, vol. 36, p. 1727, 1974.
[43] G. V. Khazanov, M. A. Koen and S. I. Burenkov, "A numerical solution to the kinetic equation for photoelectrons taking into account the free and trapped zones," *Cosmic Res.*, vol. 17, p. 894, 1979*b*.
[44] A. E. S. Green and T. Sawada, "Ionization cross-section and secondary electron distribution," *J. Atmos. Terr. Phys.*, vol. 34, p. 1719, 1972.
[45] A. E. S. Green and R. S. Stolarski, "Analytical models of electron impact excitation cross-sections," *J. Atmos. Terr. Phys.*, vol. 34, p. 1703, 1972.
[46] M. E. Riley, C. J. McCallum and F. Biggs, *Atom Data and Nucl. Data Tables*, vol. 15, p. 443, 1975.
[47] L. G. Jacchia, "Received static models of the thermosphere and exosphere with empirical temperature profiles," *SAO, Spec. Rep.*, p. 332, 1971.
[48] G. P. Mantas, "Electron collision processes in the ionosphere," *Aeron. Rep.*, p. 54, 1973.
[49] R. J. Cicerone, W. E. Swartz, R. S. Stolarski, A. F. Nagy and J. S. Nisbet, "Thermalization and transport of photoelectrons: a comparison of theoretical approaches," *J. Geophys. Res.*, vol. 78, p. 6709, 1973.
[50] J. S. Nisbet, "Photoelectron escape from the ionosphere," *J. Atmos. Terr. Phys.*, vol. 30, p. 1257, 1968.
[51] W. E. Swartz, *Sci. Rept. 381, Ionosphere Res. Lab., Pa. State Univ.*, 1972.
[52] J. D. Winningham, D. T. Decker, J. V. Kozyra, J. R. Jasperse and A. F. Nagy, "Energetic (¿ 60 eV) atmospheric photoelectrons," *J. Geophys. Res.*, vol. 94, p. 15335, 1989.
[53] G. V. Khazanov, T. I. Gombosi, A. F. Nagy and M. A. Koen, "Analysis of the ionosphere-plasmasphere transport of superthermal electrons, 1, Transport in the plasmasphere," *J. Geophys. Res.*, vol. 97, p. 16887, 1992.
[54] G. V. Khazanov, M. A. Koen and S. I. Burenkov, "Kinetic equation for plasmaspheric photoelectrons which is averaged over oscillations between the points of reflection," *Cosmic Research*, vol. 17, p. 466, 1979*a*.
[55] I. P. Shkarofsky, T. W. Johnston and M. P. Bachynski, *The Particle Kinetics of Plasmas*. London: Addison-Wesley, 1966.
[56] A. B. Gurevich, "," *Nonlinear Phenomena in the Ionosphere*. New York: Springer-Verlag, 1978.
[57] N. Mott and G. Messy, "Atom collision theory," *Mir*, 1969.
[58] W. F. Hoegy, J. P. Fournier and E. G. Fontheim, "Photoelectron energy distribution in the F-region," *J. Geophys. Res.*, vol. 70, p. 5464, 1965.
[59] V. D. Sivukhin, *Reviews of Plasma Physics*, vol. 1, New York: Consultants Bureau, 1965.

George V. Khazanov was born in 1948. He received the M.S. and the Ph.D. degrees from the Irkutsk State University, Irkutsk, Russia, in 1971 and 1974, respectively.

From 1976 to 1984 he was the Head of Ionospheric Plasma Physics Laboratory of the Irkutsk State University. From 1985 to 1991 he was Professor, Chairman of Theoretical Physics Department and Dean of Physical Faculty of Altai State University, Barnaul, Russia. In 1991 he joined the research staff of Space Physics Research Laboratory at the University of Michigan, Ann Arbor, MI. His research interests include theoretical space plasma physics, superthermal particle transport, and modeling of high speed plasma flows in ionosphere and magnetosphere. He is the author or co-author of five monographs and over one hundred and seventy scientific publications and more than one hundred and fifty seminars and conference papers.

Torsten Neubert was born in Copenhagen, Denmark, on August 16, 1950. He received the M.Sc. degree in electronic engineering from the Technical University of Denmark in 1976, and in 1981 the Ph.D. degree from the University of Copenhagen for studies carried out at the Danish Space Research Institute.

After his thesis work, he continued at the Danish Space Research Institute, studying natural and spacecraft induced plasma wave and particle phenomena. In 1984 he joined the Space Telecommunications and Radioscience Laboratory at Stanford University, first as a postdoctoral fellow and, in 1987, as an Associate Research Scientist. At Stanford he studied plasma wave radiation and particle dynamics as observed in active electron beam, plasma and neutral gas ejection experiments flown on the space shuttle (STS-3, Spacelab 1 and 2) and on sounding rockets (CHARGE-2). In 1990 he accepted a position as Associate Research Scientist at the Space Physics Research Laboratory, University of Michigan, where he continues studies related to active experiments. His current interests include PIC simulations of electron beams and plasma flows.

Dr. Neubert is a member of the American Geophysical Union.

Grigorii D. Gefan, photograph and biography not available at time of publication.